JAMES | Journal of Advances in Modeling Earth Systems®

RESEARCH ARTICLE
10.1029/2020MS002412

Key Points:

- The large scale response in an uncoupled atmospheric simulation is the response of the model rather than that of the atmosphere
- A coupled modeling approach is necessary to investigate the large scale atmospheric response to mesoscale sea surface temperature variability
- A pair of oceanic heat fluxes that do not have large scale differences is critical to produce a realistic large scale atmospheric response

Correspondence to:
I. Szunyogh,
szunyogh@tamu.edu

Citation:
Szunyogh, I., Forinash, E., Gyarmati, G., Jia, Y., Chang, P., & Saravanan, R. (2021). Evaluation of a coupled modeling approach for the investigation of the effects of SST mesoscale variability on the atmosphere. *Journal of Advances in Modeling Earth Systems*, *13*, e2020MS002412. https://doi.org/10.1029/2020MS002412

Received 16 NOV 2020
Accepted 30 AUG 2021

© 2021 The Authors. Journal of Advances in Modeling Earth Systems published by Wiley Periodicals LLC on behalf of American Geophysical Union. This is an open access article under the terms of the Creative Commons Attribution-NonCommercial-NoDerivs License, which permits use and distribution in any medium, provided the original work is properly cited, the use is non-commercial and no modifications or adaptations are made.

Evaluation of a Coupled Modeling Approach for the Investigation of the Effects of SST Mesoscale Variability on the Atmosphere

Istvan Szunyogh[1], Eric Forinash[1], Gyorgyi Gyarmati[1], Yinglai Jia[2], Ping Chang[1,3], and R. Saravanan[1]

[1]Department of Atmospheric Sciences, Texas A&M University, College Station, TX, USA, [2]Physical Oceanography Laboratory Ocean University of China, Qingdao, China, [3]Department of Oceanography, Texas A&M University, College Station, TX, USA

Abstract This study further evaluates the modeling approach of Jia et al. (2019), https://doi.org/10.1029/2019gl081960 (JEA19) to investigate the potential effects of mesoscale sea surface temperature (SST) variability on the atmospheric circulation. The approach employs a global atmospheric circulation model coupled to a slab ocean model to produce two ensembles of simulations: one in which the SST exhibits realistic mesoscale variability, and another in which the mesoscale SST variability is suppressed. The results of the present study suggest that the modeling approach yields the desired SST differences between the two ensembles at the mesoscales. They also show, however, that the approach can lead to undesirable SST differences at the large scales, if the prescribed pair of oceanic heat flux fields have large scale differences. In the experiments of JEA19, such forced, large scale SST differences dominate over the large scale differences that may develop in response to changes in the large scale atmospheric circulation by nonlinear interactions with the SST. This result suggests that finding a proper pair of estimates of the oceanic heat flux fields is necessary for the investigation of the potential upscale impact of mesoscale SST variability on the atmosphere by the approach of JEA19. The paper concludes with proposing a potential improved strategy to obtain such a pair of estimates.

Plain Language Summary This study evaluates a modeling approach to investigate the potential effects of mesoscale (scales smaller than 100 km) ocean sea surface temperature (SST) variability on the atmospheric circulation. The approach employs a global atmospheric circulation model coupled to a thermodynamical model of the ocean. Two ensembles of model simulations are prepared: one in which the ocean exhibits realistic mesoscale SST variability, and another in which that variability is suppressed. The results suggest that the modeling approach yields the desired mesoscale SST differences. They also show, however, that the approach can lead to undesirable large scale SST differences, if there are large scale differences between the prescribed oceanic heat transport fields of the two ensembles. In the experiments of JEA19, such forced, large scale SST differences dominate over the large scale differences that may develop in response to changes in the large scale atmospheric circulation by two-way interactions with the SST. This result suggests that finding a proper pair of estimates of the oceanic heat transport fields is necessary for the investigation of the potential upscale impact of mesoscale SST variability on the atmosphere by the approach of JEA19. The paper concludes with proposing a potential improved strategy to obtain such a pair of estimates.

1. Introduction

It is well established that the large-scale oceanic fronts associated with the Kuroshio Extension and the Gulf Stream anchor the entrance regions of the midlatitude atmospheric storm tracks of the Northern Hemisphere (e.g., Nakamura et al., 2004, 2008). It is also widely accepted that the SST anomalies associated with the ocean mesoscale eddies that form along the large scale oceanic fronts have a major effect on the atmospheric boundary layer (e.g., Chelton & Xi, 2010; Small et al., 2008; Xie, 2004). The deeper tropospheric effects of SST mesoscale variability, however, are less understood and have been the subject of ongoing research. For instance, Woollings et al. (2010) found a subtle, but significant effect on the midlatitude storm tracks in simulations with a limited area version of the Hadley Center's third generation atmospheric model.

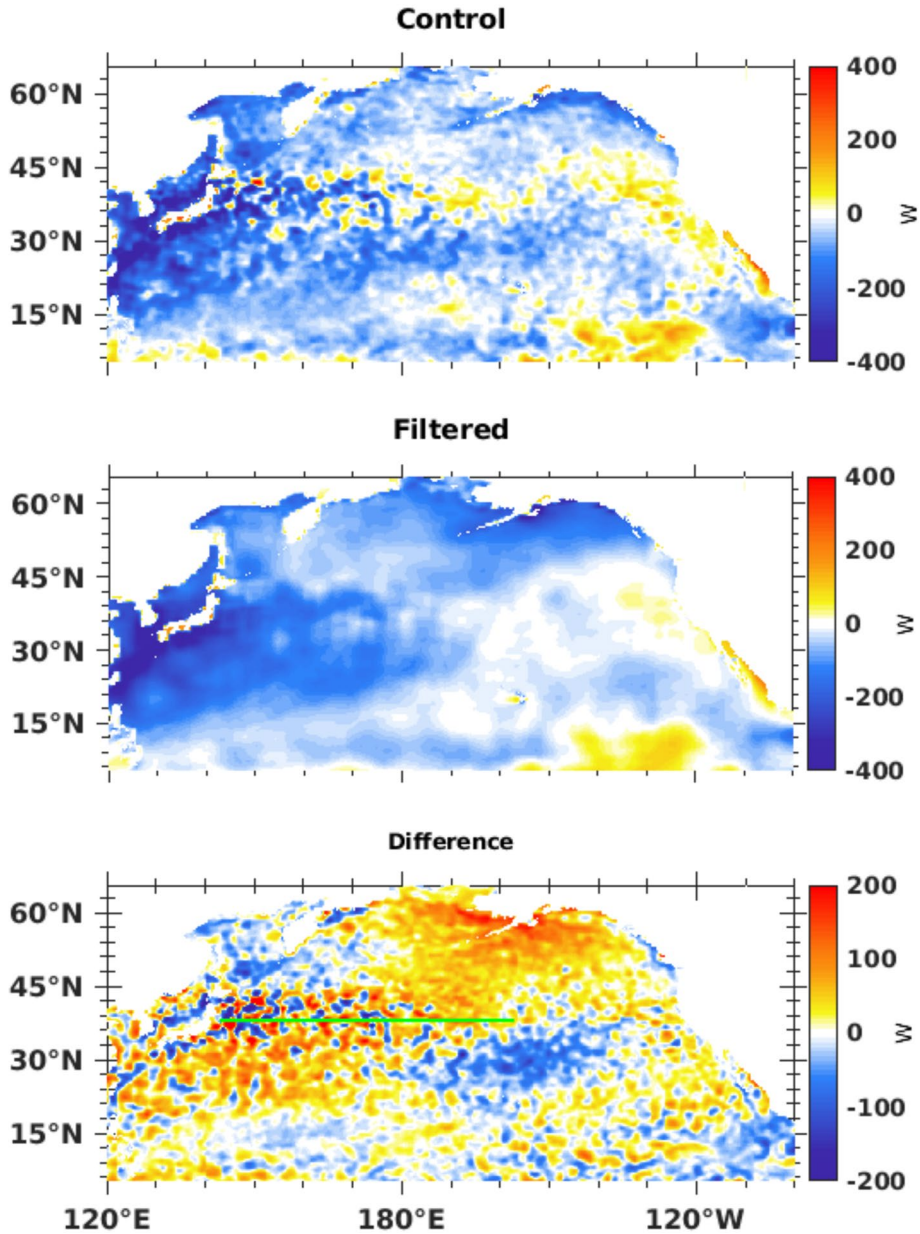

Figure 1. The $Q_{slab}(\mathbf{r})$ estimates of the oceanic heat flux used in the two ensembles. Shown are (color shades; top) $Q^{c}_{slab}(\mathbf{r})$ and (middle) $Q^{f}_{slab}(\mathbf{r})$. A negative (positive) value indicates heating (cooling) of the ocean mixed layer. Also shown (bottom) is the differences $\Delta Q_{slab}(\mathbf{r})$ between the two estimates. The green line segment along 38°N indicates the position of the Kuroshio Extension.

Ma et al. (2015, 2017) reported a poleward shift of the North Pacific storm track, with a deep tropospheric impact that extended to the west coast of North America, in atmospheric simulations with the limited area Weather Research and Forecasting (WRF) model. Foussard et al. (2019) also found a polar shift of the storm track in idealized midlatitude channel model experiments with WRF, while Zhang et al. (2020) observed it in global atmospheric simulations with an earlier version of the Community Atmosphere Model (CAM4).

The aforementioned findings suggest that ocean mesoscale variability has a potentially significant deep tropospheric effect on the atmospheric circulation. The implications of the existence of such an effect would be important for both climate modeling and numerical weather forecasting. For instance, the ocean mesoscale eddies that form along the midlatitude oceanic fronts can persist for months (Chelton et al., 2004) and

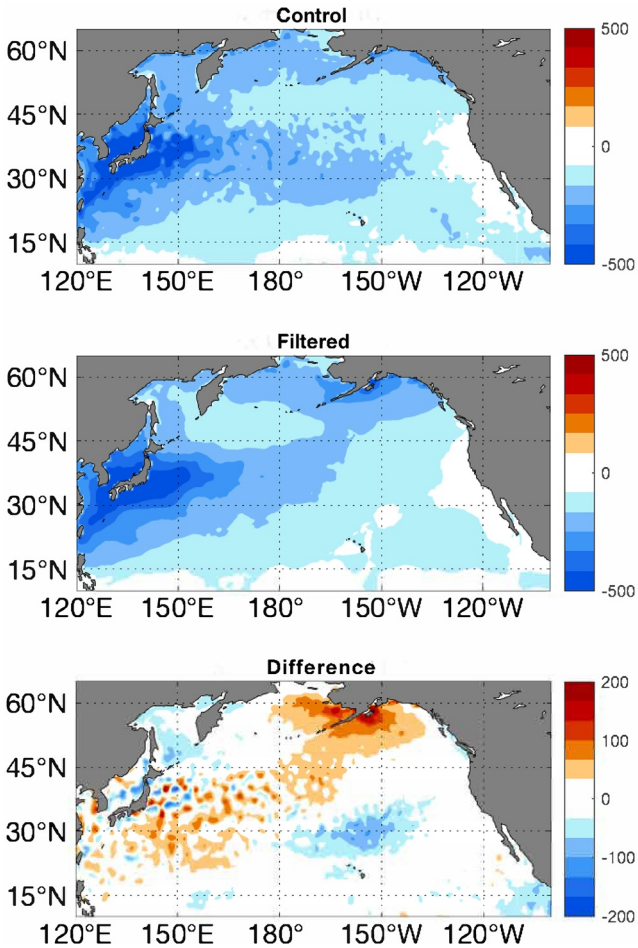

Figure 2. The atmospheric heat fluxes computed from the uncoupled atmospheric simulations. Shown are $\overline{Q_{atm}}^{t,e}(\mathbf{r})$ for (color shades) (top) the unfiltered sea surface temperature (SST), and (middle) filtered SST. A negative (positive) value indicates heating (cooling) of the ocean mixed layer. Also shown (bottom) is the differences $\Delta\overline{Q_{atm}}^{t,e}(\mathbf{r})$ between the two estimates.

may serve as a potential source of atmospheric predictability in the subseasonal-to-seasonal (S2S) time range (Saravanan & Chang, 2018). (Identifying sources of S2S predictability has been an active area of research in recent years (e.g., Lang et al., 2020; Mariotti et al., 2020).

The potential importance of the atmospheric effects of ocean mesoscale variability motivates the search for coupled atmosphere-ocean modeling approaches that could replace the current uncoupled, atmosphere-only modeling experiment designs to explore them. The two main challenges that a coupled approach must address are the extremely high computational cost of a fully coupled simulation at the required resolution and the large systematic errors (biases) that tend to develop in the ocean component of such a simulation. Jia et al. (2019) (JEA19 hereafter), with these challenges in mind, proposed the use of a high-resolution slab ocean model in the coupled simulations. This approach has a number of conceptually appealing features. First, the computational cost of the coupled simulations with a slab ocean model is significantly lower than that with a full ocean circulation model. Second, it can still simulate the nonlinear thermodynamical feedback between the atmosphere and ocean, eliminating the implicit assumption of the atmosphere-only modeling approaches that the heat capacity of the ocean is infinite, while it can also account for the oceanic heat transport by a prescribed oceanic heat flux field. Third, systematic SST errors (biases) are easier to control in a slab ocean model than a full ocean circulation model (Zuidema, 2016). Finally, in a potential operational forecast application, which requires the availability of real-time initial conditions for all prognostic model variables, it requires the availability of only an SST analysis for the ocean.

In their demonstration of the proposed approach, JEA19 carried out global simulation experiments with the Community Earth System Model (CESM) of the National Center for Atmospheric Research (NCAR). Our goal is to further analyze the simulation results of JEA19, with the hope that the investigation can lead to refinements of the modeling approach. While the simulations are global, we focus our attention on the dynamical processes of the North Pacific. The structure of the paper is as follows. Section 2 describes the design of the simulations of JEA19, with a special attention to the procedure for the estimation of the prescribed oceanic heat flux fields of the slab ocean model. Section 3 presents the diagnostic results, while Section 4 draws the conclusions and proposes potential improvements to the design of the simulations.

2. Background

We first describe the prognostic equation of the slab ocean model, which governs the spatiotemporal evolution of the SST. We then explain the approach of JEA19 for the estimation of the oceanic heat flux, which is a prescribed input field of the slab ocean model. We continue with an explanation of the approach of JEA19 to simulate the effect of ocean mesoscale variability on the atmospheric circulation by two ensembles of simulations: one in which the SST mesoscale variability is retained and another in which the SST mesoscale variability is suppressed. We refer to the former ensemble as the *control ensemble*, and the latter as the *filtered ensemble*.

2.1. The Slab Ocean Model

A slab ocean model consists of a single mixed layer whose thermodynamical state depends on the horizontal location $\mathbf{r}$ and time t. The thermal effects of the oceanic heat transport on the mixed layer are accounted

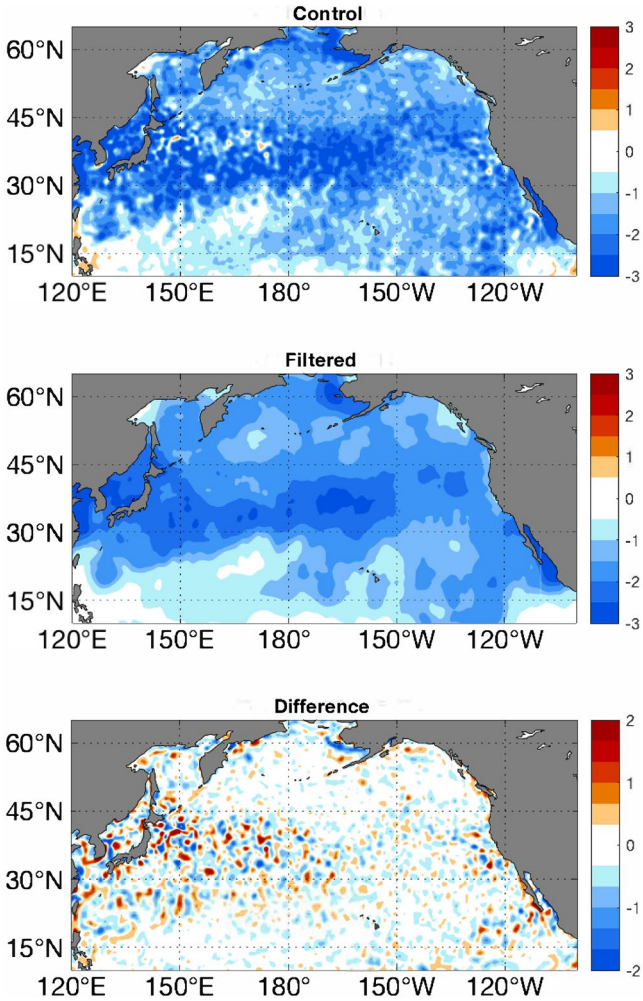

Figure 3. The change in the sea surface temperature (SST) analyses over the one month simulation period. Shown are $T^a_{mix}(\mathbf{r},t_0+M)-\Delta T^a_{mix}(\mathbf{r},t_0)$ for (color shades; top) the unfiltered SST, and (middle) filtered SST. A negative (positive) value indicates heating (cooling) of the ocean mixed layer. Also shown (bottom) is the differences $\Delta T^a_{mix}(\mathbf{r},t_0+M)-\Delta T^a_{mix}(\mathbf{r},t_0)$ between the two fields.

for by the $Q_{ocn}(\mathbf{r},t)$ net outgoing heat flux at the bottom and side walls of the water column. The single prognostic equation of the model is

$$\frac{\partial T_{mix}}{\partial t}(\mathbf{r},t)=\frac{1}{\rho c_o h_{mix}(\mathbf{r})}\Big[Q_{atm}(\mathbf{r},t)-Q_{ocn}(\mathbf{r},t)\Big], \tag{1}$$

where $T_{mix}(\mathbf{r},t)$ is the SST (the temperature of the ocean mixed layer), ρ is the constant density of ocean water, c_o is the specific heat of ocean water, $h_{mix}(\mathbf{r})$ is the depth of the ocean mixed layer, $Q_{atm}(\mathbf{r},t)$ is the incoming heat flux from the atmosphere, and $Q_{ocn}(\mathbf{r},t)$ is the prescribed estimate of the net outgoing oceanic heat flux. For brevity, we will refer to $Q_{atm}(\mathbf{r},t)$ as the *atmospheric heat flux*, and to $Q_{ocn}(\mathbf{r},t)$ as the *oceanic heat flux*. (A negative value of $Q_{ocn}(\mathbf{r},t)$ indicates heating of the mixed layer, while a positive value indicates cooling.) In the experiments of JEA19, the parameters of Equation 1 were $\rho=1026\,\mathrm{kgm}^{-3}$, $c_0=3930\,\mathrm{Jkg}^{-1}\mathrm{K}^{-1}$, and $h_{mix}(\mathbf{r})$ was prescribed from the Levitus (1982) Climatological Atlas of the World Ocean.

2.2. Estimation of the Oceanic Heat Flux

When a slab ocean model is coupled to the atmospheric model, the oceanic heat flux $Q_{ocn}(\mathbf{r},t)$ replaces the SST as the field that represents the thermal forcing by the ocean. If analyses (observation based estimates) of the oceanic heat flux were available, they could be used the same way in the coupled model as SST analyses used in the uncoupled atmospheric models. Because such analyses of the oceanic heat flux are not readily available, the implementation of a slab ocean model requires the use of some technique for the estimation of the oceanic heat flux. JEA19 obtained estimates of $Q_{ocn}(\mathbf{r},t)$ by first computing

$$Q_{atm}(\mathbf{r},t)=Q_{sol}(\mathbf{r},t)-Q_{long}(\mathbf{r},t)-Q_{sen}(\mathbf{r},t)-Q_{latent}(\mathbf{r},t) \tag{2}$$

from a 10-member ensemble of uncoupled atmospheric simulations with CESM that were forced by observations-based SST analyses. In Equation 2, $Q_{sol}(\mathbf{r},t)$ is the net radiative heating of the ocean mixed layer by solar radiation, $Q_{long}(\mathbf{r},t)$ is the net long-wave radiative cooling of the ocean mixed layer, $Q_{sen}(\mathbf{r},t)$ is the net sensible heat flux from the ocean to the atmosphere, and $Q_{latent}(\mathbf{r},t)$ is the net latent heat flux from the ocean to the atmosphere. It is important to point out that $Q_{atm}(\mathbf{r},t)$ depends nonlinearly on the SST, $T_{mix}(\mathbf{r},t)$.

The initial conditions of the 10-member ensemble were independent of each other, but all members were forced by the same time series of SST and ice analyses: 0.25° spatial resolution, daily, 0000 UTC NOAA Optimum Interpolation Sea Surface Temperature and ICE (OISSTV2) analyses from December 2007. The particular time period was chosen, because it was the time of an unstable epoch of the Kuroshio Extension that produced active mesoscale ocean eddies and strong mesoscale SST anomalies, but was also a time when the El Niño-Southern Oscillation (ENSO) and the Pacific Decadal Oscillation (PDO) were nearly neutral. It was also the period investigated by Ma et al. (2015, 2017).

After computing $Q_{atm}(\mathbf{r},t)$ for each member of the ensemble of uncoupled atmospheric simulations, JEA19 computed $Q_{ocn}(\mathbf{r},t)$ for each member from Equation 1, using finite-differences to approximate the SST tendencies from the SST analyses. Finally, they computed the average of $Q_{ocn}(\mathbf{r},t)$ over all ensemble members and times to obtain a time-independent estimate $Q_{slab}(\mathbf{r})$ of $Q_{ocn}(\mathbf{r},t)$. This static estimate was used as the prescribed input field $Q_{ocn}(\mathbf{r},t)$ of Equation 1 at all times in the coupled simulations, that is, the actual prognostic equation of the slab ocean model was

$$\frac{\partial T_{mix}}{\partial t}(\mathbf{r},t)=\frac{1}{\rho c_o h_{mix}(\mathbf{r})}\Big[Q_{atm}(\mathbf{r},t)-Q_{slab}(\mathbf{r})\Big]. \tag{3}$$

The estimate $Q_{slab}(\mathbf{r})$ depends on the monthly mean atmospheric heat flux, $\overline{Q_{atm}}^{t}(\mathbf{r})$. This property follows from the equation

$$\overline{Q_{ocn}}^{t}(\mathbf{r}) = \overline{Q_{atm}}^{t}(\mathbf{r}) - \rho c_0 h_{mix}(\mathbf{r})\overline{\delta T^{a}_{mix}}^{t}(\mathbf{r}), \tag{4}$$

which we obtain by taking the time mean of Equation 1 and introducing the notations

$$\overline{Q_{ocn}}^{t}(\mathbf{r}) = \frac{1}{M}\int_{t_0}^{t_0+M} Q_{ocn}(\mathbf{r},t)dt, \tag{5}$$

$$\overline{Q_{atm}}^{t}(\mathbf{r}) = \frac{1}{M}\int_{t_0}^{t_0+M} Q_{atm}(\mathbf{r},t)dt, \tag{6}$$

$$\overline{\delta T^{a}_{mix}}^{t}(\mathbf{r}) = \frac{1}{M}\int_{t_0}^{t_0+M} \frac{\partial T_{mix}}{\partial t}(\mathbf{r},t)dt = \frac{1}{M}\Big[T^{a}_{mix}(\mathbf{r},t_0+M) - T^{a}_{mix}(\mathbf{r},t_0)\Big], \tag{7}$$

where t_0 is the time at the beginning of the uncoupled simulations, M is one month, and $T^{a}_{mix}(\mathbf{r},t_0+M)$ and $T^{a}_{mix}(\mathbf{r},t_0)$ are, respectively, the SST analyses at the end and beginning of the simulations. Because $Q_{slab}(\mathbf{r})$ is the ensemble mean of $\overline{Q_{ocn}}^{t}(\mathbf{r})$ and ensemble averaging has no effect on the second term of the right-hand side of Equation 4,

$$Q_{slab}(\mathbf{r}) = \overline{Q_{atm}}^{t,e}(\mathbf{r}) - \rho c_0 h_{mix}(\mathbf{r})\overline{\delta T^{a}_{mix}}^{t}(\mathbf{r}), \tag{8}$$

where $\overline{Q_{atm}}^{t,e}(\mathbf{r})$ is the ensemble mean of $\overline{Q_{atm}}^{t}(\mathbf{r})$.

2.3. The Control and Filtered Experiment

JEA19 carried out two 10-member ensembles of uncoupled atmospheric simulations to obtain a pair of estimates of $Q_{slab}(\mathbf{r})$. In these simulations, the atmospheric and slab ocean model both had horizontal resolution 0.23° × 0.23°, while the atmospheric model had 30 vertical levels. The two ensembles differed in the treatment of the SST analyses that were used to compute the two estimates of $Q_{slab}(\mathbf{r})$: one used 0.23° × 0.23° resolution SST analyses, while the other used the same SST analyses after filtering the mesoscale variability by a 5° × 5° boxcar averaging filter. The same sets of unfiltered and filtered SST analyses were used, in combination with the corresponding values of $\overline{Q_{atm}}^{t,e}(\mathbf{r})$, to approximate the left-hand side of Equation 1 for the computation of $Q_{slab}(\mathbf{r})$. This procedure yielded the two estimates of $Q_{slab}(\mathbf{r})$: $Q^{c}_{slab}(\mathbf{r})$ for the unfiltered SST analyses, and $Q^{f}_{slab}(\mathbf{r})$ for the filtered SST analyses (Hereafter, a superscribed c or f, respectively, indicates a scalar field of the control or filtered simulations.).

JEA19 carried out two ensembles of coupled simulations: one that used $Q^{c}_{slab}(\mathbf{r})$ and the unfiltered SST analysis from 0000 UTC, December 1, 2007 as the SST initial condition, and another that used $Q^{f}_{slab}(\mathbf{r})$ and the filtered version of the same SST analysis as the initial condition. The two experiments used the same 30-member ensemble of atmospheric initial conditions to produce two 30-member ensembles of month long simulations (JEA19 showed that both ensembles developed a significant ensemble spread of the SST in response to the differences in the atmospheric conditions.) The ensemble based on the unfiltered SST analyses is the control ensemble, and the ensemble based on the filtered SST analyses is the filtered ensemble. We compute diagnostics for the two ensembles based on 6-hourly data from weeks 3 to 4 of the simulations. The motivation to discard the data from the first two weeks of the simulations is to reduce the effects of the initial transient behavior of the model on the diagnostics.

3. Results

We first show that the difference $\Delta Q_{slab}(\mathbf{r}) = Q^{c}_{slab}(\mathbf{r}) - Q^{f}_{slab}(\mathbf{r})$ between the two estimates of the oceanic heat flux drives both the mesoscale and large scale SST differences between the two ensembles. These large scale SST differences are the primary drivers of the large scale difference in the simulated atmospheric flow, which also lead to major differences in the simulated synoptic scale processes.

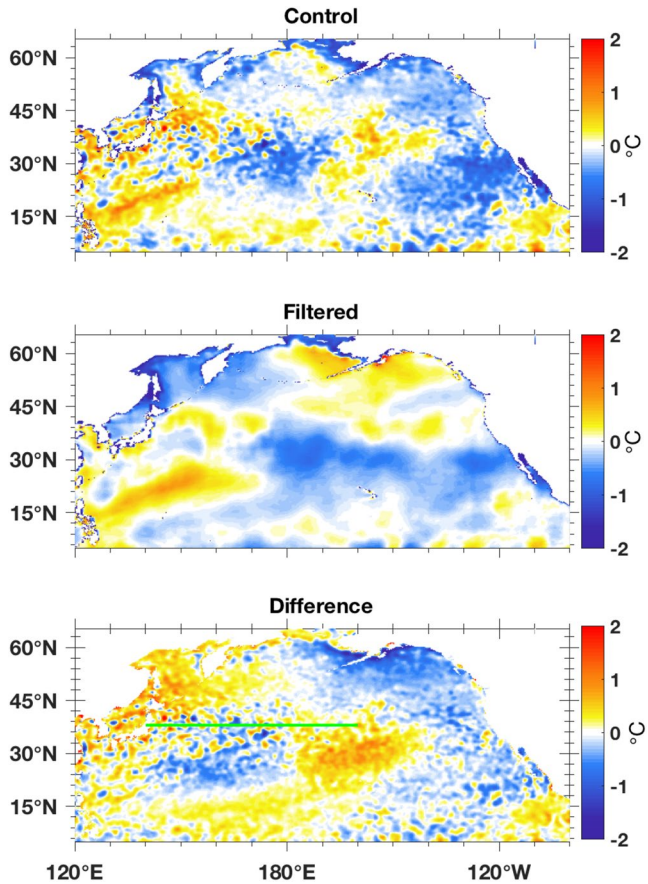

Figure 4. The mean of the differences between the sea surface temperature (SST) and the SST analysis for the two ensembles. Shown are (color shades) the systematic SST differences for (top) the control ensemble, $b^c_{mix}(\mathbf{r})$ and (middle) filtered ensemble, $b^f_{mix}(\mathbf{r})$. A negative value indicates that the mean SST is lower (higher) in the simulations than the analyses. Also shown (bottom) is the difference $b^c_{mix}(\mathbf{r}) - b^f_{mix}(\mathbf{r})$ between the fields of the top two panels. The green line segment along 38°N indicates the position of the Kuroshio Extension.

3.1. The Estimates of the Oceanic Heat Flux Field

The top two panels of Figure 1 show the $Q^c_{slab}(\mathbf{r})$ (top panel) and $Q^f_{slab}(\mathbf{r})$ (middle panel) estimates of the oceanic heat flux for the North Pacific. As can be expected, the boundaries between the regions of positive and negative values are sharper, and the absolute values of the local maxima and minima are larger in the control than the filtered experiment.The dominantly negative values of the two estimates indicate that oceanic heat transport is dominantly a heat source for the mixed layer for the winter-time oceanic conditions of the experiments. The exception is the narrow region of positive values off the coast of North America along the California Current, where oceanic heat transport is a net sink of heat for the mixed layer.

If the uncoupled atmospheric simulations produced a pair of estimates $Q^c_{slab}(\mathbf{r})$ and $Q^f_{slab}(\mathbf{r})$ that is consistent with the assumption that there are only mesoscale differences between the oceans of the two simulations, the difference $\Delta Q_{slab}(\mathbf{r})$ (bottom panel of Figure 1) would only have mesoscale components. The fact that $\Delta Q_{slab}(\mathbf{r})$ has apparent large scale components indicates that the pair of estimates of JEA19 is not consistent with this assumption. To investigate the origin of this inconsistency, we consider the equation

$$\Delta Q_{slab}(\mathbf{r}) = \Delta\overline{Q_{atm}}^{t,e}(\mathbf{r}) - \frac{\rho c_0 h_{mix}(\mathbf{r})}{M}\Big[\Delta T^a_{mix}(\mathbf{r},t_0+M) - \Delta T^a_{mix}(\mathbf{r},t_0)\Big], \quad (9)$$

where

$$\Delta T^a_{mix}(\mathbf{r},t_0+M) = T^{ac}_{mix}(\mathbf{r},t_0+M) - T^{af}_{mix}(\mathbf{r},t_0+M), \quad (10)$$

$$\Delta T^a_{mix}(\mathbf{r},t_0) = T^{ac}_{mix}(\mathbf{r},t_0) - T^{af}_{mix}(\mathbf{r},t_0), \quad (11)$$

Equation 9 follows directly from Equation 8. The second term of the right-hand side of Equation 9 has only mesoscale components, because it represents the contribution of the changes in the analyzed SST mesoscale anomalies over the month. Thus the source of the large scale components of $\Delta Q_{slab}(\mathbf{r})$ must be the $\Delta\overline{Q_{atm}}^{t,e}(\mathbf{r})$ mean difference between the atmospheric heat fluxes computed from the two ensembles of uncoupled simulations. A comparison of $\Delta\overline{Q_{atm}}^{t,e}(\mathbf{r})$ (Figure 2, bottom panel) and $\Delta T^a_{mix}(\mathbf{r},t_0+M) - \Delta T^a_{mix}(\mathbf{r},t_0)$ (Figure 3, bottom panel) confirms this conclusion.

Finding a large scale response of the atmospheric heat flux to ocean mesoscale variability in the uncoupled atmospheric simulations is not unexpected based on the results of the earlier studies (Foussard et al., 2019; Ma et al., 2015, 2017). It is also possible that a similar response exists in nature, considering the nonlinearity of the interactions between $Q_{atm}(\mathbf{r},t)$ and $T_{mix}(\mathbf{r},t)$. It is important to notice, however, that such a response is not consistent with the physical assumptions made implicitly by using an uncoupled atmospheric model for the simulations. In particular, because the thermodynamical equation for the mixed layer (Equation 1) is satisfied by nature, large scale patterns of $Q_{atm}(\mathbf{r},t)$ can exist only if there are matching large scale patterns of SST changes. If the only difference between the two model oceans is the presence of mesoscale variability in one of them, $Q_{ocn}(\mathbf{r},t)$ has only mesoscale components that cannot cancel out the large scale components of $Q_{atm}(\mathbf{r},t)$. But, such large scale patterns of SST changes are not consistent with the SST forcing fields used in the uncoupled simulations. This argument motivates us to interpret the large scale component of $\Delta\overline{Q_{atm}}^{t,e}(\mathbf{r})$ computed from uncoupled atmospheric simulations as the *response of the particular atmospheric model* to ocean mesoscale variability rather than the response of the atmosphere in nature. In other words, the large scale components of $\overline{Q_{atm}}^{t,e}(\mathbf{r})$ represent differences between the biases of the uncoupled simulations. In particular, the filtered simulations are likely to be biased, because they cannot account for the atmospheric heat fluxes associated with mesoscale SST variability. But, in a model

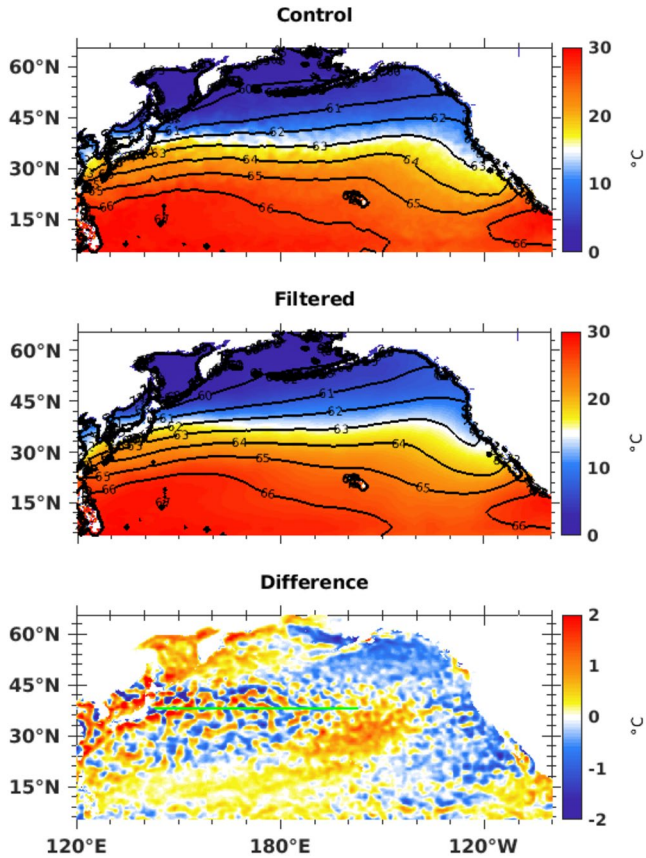

Figure 5. The mean sea surface temperature (SST) field for the two ensembles. Shown are (color shades) $\overline{T}^{t,e}_{mixed}(\mathbf{r})$ and (contours with interval 1 gpm) $\overline{z}^{t,e}(\mathbf{r})$ at 992 hPa for the (top) control experiment and (middle) filtered experiment. Also shown (bottom) is the differences $\Delta\overline{T}^{t,e}_{mixed}(\mathbf{r})$ between the SST fields of the top two panels. The green line segment along 38°N indicates the position of the Kuroshio Extension.

tuned for scenarios in which mesoscale SST variability is not present, the parameterization schemes may compensate for the effects of the lack of the heat fluxes associated with mesoscale SST variability, causing biases when the mesoscale SST variability is resolved. Most likely, bothof these factors contribute to the large scale components of $\overline{Q_{atm}}^{t,e}(\mathbf{r})$.

The appeal of using a slab ocean model for the investigation of the effects of mesoscale SST variability is that large scale patterns of $\Delta\overline{Q_{atm}}^{t,e}(\mathbf{r})$ can develop in response to the mesoscale SST variability without violating the thermodynamical equation for the ocean mixed layer. Large scale differences between the atmospheric heat fluxes of the two ensembles inevitably lead to large scale SST differences, which in turn would modulate the large scale difference between the atmospheric heat fluxes. The goal of the modeling approach of JEA19 is exactly to detect the large scale differences in the atmospheric circulation and SST that result from this nonlinear process.

What is the effect of the undesirable large scale components of $\Delta Q_{slab}(\mathbf{r})$ on the coupled simulations? We start the discussion of this problem with an examination of the mean differences,

$$b^{c}_{Tmix}(\mathbf{r}) = \overline{T^{c}_{mix}(\mathbf{r},t) - T^{ac}_{mix}(\mathbf{r},t)}^{t,e}, \quad (12)$$

$$b^{f}_{Tmix}(\mathbf{r}) = \overline{T^{f}_{mix}(\mathbf{r},t) - T^{af}_{mix}(\mathbf{r},t)}^{t,e}, \quad (13)$$

between the simulated and analyzed SST fields of the two ensembles of coupled simulations (Figure 2). Here, $T^{ac}_{mix}(\mathbf{r},t)$ and $T^{af}_{mix}(\mathbf{r},t)$ are the unfiltered and filtered SST analyses, respectively. We emphasize that, in principle, $b^{c}_{Tmix}(\mathbf{r})$ and $b^{f}_{Tmix}(\mathbf{r})$ do not have be zero, because nonlinear effects in the evolution of the SST, which are introduced by the nonlinear feedback from the atmosphere, can lead to systematic differences between the simulated and analyzed SST. Thus the large scale patterns of small magnitude systematic differences (less than 1.0°C at most locations) in the top two panels of Figure 2 are not causes for concern at first sight. But, a comparison of the bottom panels of Figures 1 and 2 suggests that the large scale patterns of the difference $b^{c}_{Tmix}(\mathbf{r}) - b^{f}_{Tmix}(\mathbf{r})$ closely resemble the large scale patterns of $\Delta Q_{slab}(\mathbf{r})$ with the opposite signs. This relationship between the two fields suggests that the mean differences between the SST fields of the coupled simulations and the analyses are dominantly driven by $\Delta Q_{slab}(\mathbf{r})$ rather than the nonlinear interactions between the SST and the atmosphere.

3.2. Mean SST, and the Mean Atmospheric Flow

The mean SST fields of the two ensembles (Figure 5, top two panels) and their difference (Figure 5, bottom panel) show that JEA19 achieved their goal to maintain the SST mesoscale variability in the control ensemble and suppress it in the filtered ensemble. Most importantly, the SST mesoscale anomalies associated with the mesoscale eddies of the Kuroshio Extension (west of the dateline along the green line segment in the figure) are clearly present in the SST difference field $\Delta\overline{T}^{t,e}_{mix}(\mathbf{r})$. Elsewhere, however, the large scale differences dominate, which is not surprising in light of the results shown in Figure 4, considering that

$$\Delta\overline{T}^{t,e}_{mix}(\mathbf{r}) = \left[b^{c}_{mix}(\mathbf{r}) - b^{f}_{mix}(\mathbf{r})\right] + \overline{T^{ac}_{mix}(\mathbf{r},t) - T^{af}_{mix}(\mathbf{r},t)}^{t,e}. \quad (14)$$

Based on this equation, the field in the bottom panel of Figure 5 (left-hand side term) should look like the field in the bottom panel of Figure 4 (first term of the right-hand side), except for the footprints of the persistent mesoscale anomalies (second term of the right-hand side). The most important such anomalies in the North Pacific are the mesoscale eddies of the Kuroshio Extension. Because the large scale component of $\Delta Q_{slab}(\mathbf{r})$

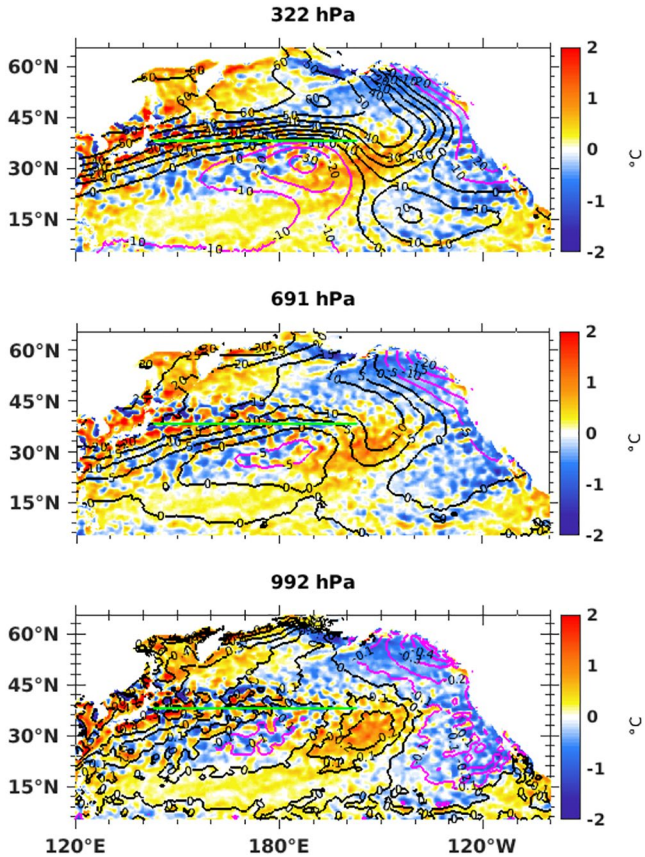

Figure 6. Illustration of the relationship between the mean sea surface temperature (SST) differences and the differences in the atmospheric mean flow in the two ensembles. Shown are (color shades) $\overline{T}^{t,e}_{mixed}(\mathbf{r})$ and (contours) the $\overline{z}^{t,e}(\mathbf{r})$ difference field at (bottom) 992 hPa, (middle) 691 hPa, and (top) 322 hPa. Black contours indicate positive, while magenta contours negative values. The contour intervals are 0.1, 5, and 10 gpm at 992, 691, and 322 hPa, respectively. The green line segment along 38°N indicates the position of the Kuroshio Extension.

drives the large scale component of $\left[b^{c}_{mix}(\mathbf{r}) - b^{f}_{mix}(\mathbf{r})\right]$, it also drives the large scale component of $\Delta\overline{T}^{t,e}_{mix}(\mathbf{r})$. From an atmospheric point of view, the close relationship between the large-scale components of $\Delta Q_{slab}(\mathbf{r})$ and $\Delta\overline{T}^{t,e}_{mix}(\mathbf{r})$ is important, because by that relationship, $\Delta Q_{slab}(\mathbf{r})$ also controls the large scale differences of the mean atmospheric flow in the lower troposphere: at location where $\Delta\overline{T}^{t,e}_{mix}(\mathbf{r})$ is higher, the mean geopotential height difference $\Delta\overline{z}^{t,e}(\mathbf{r})$ is also higher near the surface (Figure 6, bottom panel).The strong influence of $\Delta Q_{slab}(\mathbf{r})$ on the mean geopotential height field is not limited to the lower troposphere (Figure 5). In fact, the small ($|\Delta\overline{z}^{t,e}|(\mathbf{r}) \leq 4$ gpm) differences near the surface (bottom panel) translate to differences up to about 20 gpm in the middle troposphere (middle panel), and 60 gpm in the upper troposphere (top panel). This vertical profile of the geopotential height differences reflects an about 50–55 gpm difference of the atmospheric scale height, which would corresponds to a 1.7 K difference of the air temperature in an isothermal atmosphere. While the dominant large scale features of the $\Delta\overline{z}^{t,e}(\mathbf{r})$ field shift further and further to the east with height (compare the contour lines in the three panels of Figure 6), they are clearly anchored by the dominant large scale features of $\Delta\overline{T}^{t,e}_{mixed}(\mathbf{r})$, that is, the large scale features of $\Delta Q_{slab}(\mathbf{r})$.

The large scale features of $\Delta\overline{z}^{t,e}(\mathbf{r})$ have a major influence on the differences between the synoptic scale energy conversion and transport processes in the two ensembles. We demonstrate this for the North Pacific storm track, which is the region of high eddy kinetic energy (warm color shades) in the top two panels of Figure 7. The eddy kinetic energy is lower in the control experiment along and directly downstream of the Kuroshio Extension region (bottom panel). Further downstream, in the region of the relative ridge (in the mean geopotential height difference field) over the west coast, the eddy kinetic energy becomes higher in the control experiment. This spatial distribution of the eddy kinetic energy suggests that in the control experiment the upstream generation of eddy kinetic energy is reduced and its downstream propagation is modified by the differences in the large-scale atmospheric flow. (A detailed analysis of the related differences in the energy conversion processes can be found in an earlier, preprint version of the present paper (Szunyogh et al., 2021).)

4. Summary and Conclusions

We evaluated the coupled modeling approach of JEA19 to investigate the effects of SST mesoscale variability on the atmosphere. The strategy uses an Earth system model, in which the atmosphere is thermally coupled to a slab ocean, making the SST a model state variable. The strategy involves generating two ensembles of simulations, in which the model has the same mesoscale SST variability permitting resolution, but that variability is suppressed in one of them. This study is based on data from the simulation experiments of JEA19 with the NCAR CESM.

We argued that the potential advantage of the approach of JEA19 over those based on uncoupled atmospheric model simulations is that large scale atmospheric differences can develop between the two ensembles without violating the thermodynamical equation for the ocean mixed layer. This behavior becomes possible, because the slab ocean model can respond to large scale changes of the atmospheric heat flux by large scale changes of the SST. The resulting large scale SST changes would then lead to further large scale changes in the atmospheric flow. One of the primary goals of the modeling approach of JEA19 is to make the detection of the large scale changes that may result from this nonlinear process possible. We found that while the simulations of JEA19 produced the desired mesoscale SST differences, they were unable to isolate the large

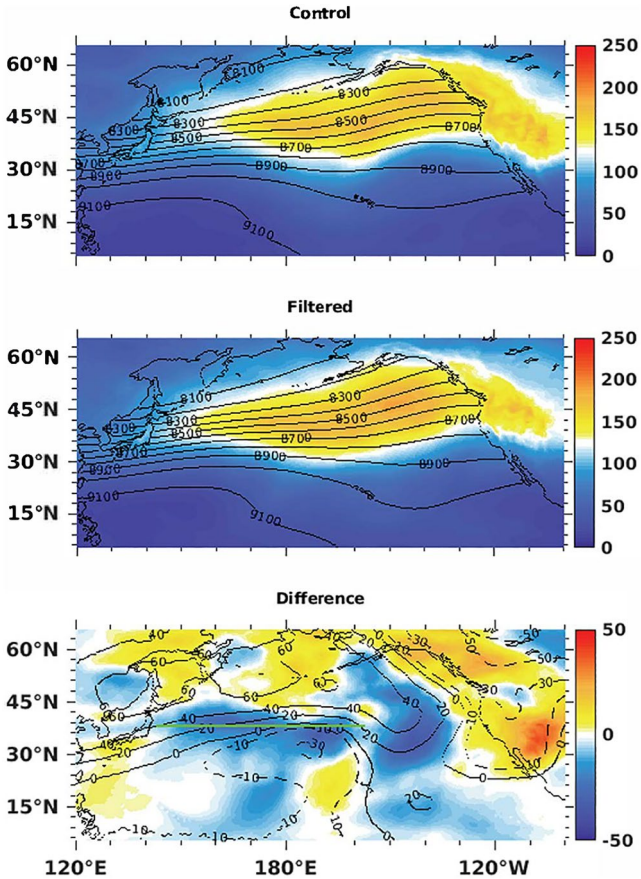

Figure 7. The vertically averaged mean eddy kinetic energy in the two ensembles. Shown are (color shades) the mean kinetic energy and (contours) $\overline{z}^{t,e}(\mathbf{r})$ at 322 hPa for (top) the control experiment and (middle) the filtered experiment. Also shown are (bottom) the differences between the fields of the top two panels. The green line segment along 38°N indicates the position of the Kuroshio Extension.

scale changes produced by nonlinear interactions between the ocean and the atmosphere. We attributed the latter to the particular method JEA19 used for the estimation of the oceanic heat flux fields.

In a slab ocean model, the oceanic heat flux is a prescribed forcing field that describes the transport of heat in the ocean. Under the assumption that the only difference between the oceans of the two ensembles is the presence of mesoscale variability in one of them, there should only be mesoscale differences between the oceanic heat fluxes of the two ensembles. The pair of estimates of the oceanic heat fluxes used by JEA19, which were obtained by uncoupled atmospheric simulations, did not satisfy this condition. Hence, the large scale SST differences between the two ensembles of coupled simulations were dominated by forced differences rather than differences that were the results of nonlinear interactions between the atmosphere and ocean. The large scale atmospheric response was driven by these forced large scale SST differences.

Our arguments thus far lead to the conclusion that the large scale atmospheric response to ocean mesoscale variability can be investigated only by coupled simulations. While there have been a number of studies (e.g., Putrasahan et al., 2013a, 2013b; Small et al., 2019) to investigate the lower tropospheric effect of ocean mesoscale variability on the atmosphere in a fully coupled framework, the natural first-step extension of the more common uncoupled approach is to employ a slab ocean model in a coupled system. Using a slab ocean model greatly reduces the computational cost and makes handling the SST biases much more manageable compared with using a full ocean circulation model. A successful strategy based on using a slab ocean model, however, must ensure that the pair of estimates of the oceanic heat flux does not introduce spurious effects into the large scale SST field. In particular, there should be no large scale differences between the two estimates. Ideally, this could be done by using mesoscale variability resolving analyses of the oceanic heat flux in the control ensemble, and filtered versions of the same analyses in the filtered ensemble. Such analyses, however, are not readily available, and a pair of estimates must be obtained by some other means.

A straightforward approach to obtain a pair of estimates that do not have large scale differences would be to obtain only one estimate by uncoupled atmospheric simulations, using unfiltered SST analyses for forcing, and then filter that estimate to obtain the other member of the pair. This pair of estimates, however, would still be affected by the biases of the uncoupled simulations. One potential approach to minimize the effect of these biases would be to use an iterative algorithm for the estimation of $Q^c_{slab}(\mathbf{r})$. In iteration k, the mean difference $b^{(k)}(\mathbf{r})$ between the simulated and analyzed SST would be computed as

$$b^{(k)}(\mathbf{r}) = \overline{T^{(k)}_{mix}(\mathbf{r},t) - T^{a}_{mix}(\mathbf{r},t)}^{t,e}, \tag{15}$$

where $T^{(k)}_{mix}(\mathbf{r},t)$ is the mean SST for the coupled simulations of iteration k. The formula

$$\begin{aligned} Q^{(k)}_{slab}(\mathbf{r}) &= Q^{(k-1)}_{slab}(\mathbf{r}) + \delta Q^{(k)}_{slab}(\mathbf{r}), \\ \delta Q^{(k)}_{slab}(\mathbf{r}) &= -\frac{2b_{Tmix}(\mathbf{r})}{M\rho c_o h_{mix}(\mathbf{r})}, \end{aligned} \tag{16}$$

would then yield an updated estimate $Q^{(k)}_{slab}(\mathbf{r})$ of the oceanic heating. The initial estimate $Q^{(0)}_{slab}$ for $k = 1$ could be computed as in JEA19, based on an ensemble of uncoupled simulations. This algorithm would eliminate the systematic differences between the simulated and analyzed SST after one iteration, if the response of $b^{(k)}(\mathbf{r})$ to the correction $\delta Q^{(k)}_{slab}(\mathbf{r})$ was linear. Even if the response would be nonlinear, which is likely to be the case, the hope is that the magnitude $|b^{(k)}(\mathbf{r})|$ of $b^{(k)}(\mathbf{r})$ would satisfy $|b^{(k)}(\mathbf{r})| < |b^{(k-1)}(\mathbf{r})|$ for at

least the first few iterations. The process would be stopped and $Q_{slab}^{(k)}(\mathbf{r})$ would become the estimate Q_{slab}^{c} once a desired small value of $|b^{(k)}(\mathbf{r})|$ was reached or the value of $|b^{(k)}(\mathbf{r})|$ could not be reduced further.

Finally, we note that future experiments investigating the atmospheric effects of SST mesoscale variability should strongly consider suppressing the SST mesoscale variability only in limited geographical regions rather than globally. Such an approach would allow for the separation of the effects of the different type ocean mesoscale anomalies (e.g., mesoscale eddies of the midlatitude oceanic fronts vs. tropical anomalies) and could also help to reduce the magnitude of the large scale SST differences. More refined filtering techniques should also be considered for the preparation of filtered SST and ocean heat flux fields, as they would allow for a more precise separation of the variability at the different scales and may lead to less artificial effects near the coast lines.

Data Availability Statement

The model simulation data of JEA that were used for this study are publicly available at https://doi.pangaea.de/10.1594/PANGAEA.897395.

Acknowledgments
This research has been conducted as part of the NOAA MAPP S2S Prediction Task Force and supported by NOAA grant NA16OAR4311082. Yinglai Jia was supported by National Key R&D Program of China (2017YFC1404101), and the Strategic Priority Research Program of the Chinese Academy of Sciences (Grant No. XDA11010203). Using an iterative algorithm for the estimation of the oceanic heat fluxes was first suggested by one of the anonymous reviewers of JEA19. The comments of the three anonymous reviewers of the present paper helped us to improve the presentation of our results substantially.

References

Chelton, D. B., Schlax, M. G., Freilich, M. H., & Milliff, R. F. (2004). Satellite measurements reveal persistent small-scale features in ocean winds. *Science*, *303*, 978–983. https://doi.org/10.1126/science.1091901

Chelton, D. B., & Xi, S. P. (2010). Coupled ocean-atmosphere interactions at oceanic mesoscales. *Oceanography*, *23*, 52–69. https://doi.org/10.5670/oceanog.2010.05

Foussard, A., Lapeyre, G., & Plougonven, R. (2019). Storm track response to oceanic eddies in idealized atmospheric simulations. *Journal of Climate*, *32*, 444–463. https://doi.org/10.1175/jcli-d-18-0415.1

Jia, Y., Chang, P., Szunyogh, I., Saravanan, R., & Bacmeister, J. T. (2019). A modeling strategy for the investigation of the effect of mesoscale SST variability on atmospheric dynamics. *Geophysical Research Letters*, *46*, 3982–3989. https://doi.org/10.1029/2019gl081960

Lang, A., Pegion, K., & Barnes, E. A. (2020). Introduction to special collection: "Bridging Weather and Climate: Subseasonal-to-seasonal (S2S) prediction". *Journal of Geophysical Research: Atmospheres*, *125*, e2019JD031833. https://doi.org/10.1029/2019jd031833

Levitus, S. (1982). *Climatological Atlas of the World Ocean*. NOAA Professional Paper 13 (p. 173). U.S. Government Printing Office, Washington D. C.

Ma, X., Chang, P., Saravanan, R., Montuoro, R., Hsieh, J.-S., Wu, D., et al. (2015). Distance influence of Kuroshio Eddies on North Pacific Weather Patterns. *Scientific Reports*, *5*, 17785. https://doi.org/10.1038/srep17785

Ma, X., Chang, P., Saravanan, R., Montuoro, R., Nakamura, D., Wu, D., et al. (2017). Importance of resolving Kuroshio front and eddy influence in simulating North Pacific storm tracks. *Journal of Climate*, *30*, 1861–1880. https://doi.org/10.1175/jcli-d-16-0154.1

Mariotti, A., Baggett, C., Barnes, E. A., Becker, E., Butler, A., Collins, D. C., et al. (2020). Windows of opportunity for skillful forecasts subseasonal to seasonal and beyond. *Bulletin of the American Meteorological Society*, *101*, E608–E625. https://doi.org/10.1175/bams-d-18-0326.1

Nakamura, H., Sampe, T., Goto, W., Ohfuchi, W., & Xie, S.-P (2008). On the importance of midlatitude oceanic frontal zones for the mean state and dominant variability in the tropospheric circulation. *Geophysical Research Letters*, *35*, L15709. https://doi.org/10.1029/2008gl034010

Nakamura, H., Sampe, T., Tanimoto, Y., & Shimpo, A. (2004). Observed associations among storm tracks, jet streams and midlatitude oceanic fronts. In C. Wang, S. P. Xie, & J. A. Carton (Eds.), *Earth's climate: The ocean-atmosphere interaction* (pp. 329–345). American Geophysical Union.

Putrasahan, D. A., Miller, A. J., & Seo, H. (2013a). Isolating mesoscale coupled ocean-atmosphere interactions in the Kuroshio Extension region. *Region Dynamics of Atmospheres and Oceans*, *63*, 60–78. https://doi.org/10.1016/j.dynatmoce.2013.04.001

Putrasahan, D. A., Miller, A. J., & Seo, H. (2013b). Regional coupled ocean-atmosphere downscaling in the Southeast Pacific: Impacts on upwelling, mesoscale air-sea fluxes, and ocean eddies. *Ocean Dynamics*, *63*, 463–488. https://doi.org/10.1007/s10236-013-0608-2

Saravanan, R., & Chang, P. (2018). Midlatitude mesoscale ocean-atmosphere interaction and its relevance to S2S prediction. In A. Robertson, & F. Vitart (Eds.), *The gap between weather and climate forecasting: Subseasonal to seasonal prediction*. Elsevier.

Small, R. J., deSzoeke, S. P., Xie, S. P., O'Neill, L., Seo, H., Song, Q., et al. (2008). Air-sea interaction over ocean fronts and eddies. *Dynamics of Atmospheres and Oceans*, *45*, 274–319. https://doi.org/10.1016/j.dynatmoce.2008.01.001

Small, R. J., Msadek, R., Kwon, Y.-O., Booth, J. F., & Zarzycki, C. (2019). Atmosphere surface storm track response to resolved ocean mesoscale in two sets of global climate model experiments. *Climate Dynamics*, *52*, 2067–2089. https://doi.org/10.1007/s00382-018-4237-9

Szunyogh, I., Forinash, E., Gyarmati, G., Jia, Y., Chang, P., & Saravanan, R. (2021). Evaluation of a coupled modeling approach for the investigation of the effects of SST mesoscale variability on the atmosphere. Preprint. https://doi.org/10.1002/essoar.10504810.1

Woollings, T., Hoskins, B., Blacjburn, M., Hassell, D., & Hodges, K. (2010). Storm track sensitivity to sea surface temperature resolution in a regional atmosphere model. *Climate Dynamics*, *35*, 341–353. https://doi.org/10.1007/s00382-009-0554-3

Xie, S. P. (2004). Satellite observations of cool ocean-atmosphere interaction. *Bulletin of the American Meteorological Society*, *85*, 274–319. https://doi.org/10.1175/bams-85-2-195

Zhang, C., Liu, H., Xie, J., Lin, P., Li, C., Yang, Q., & Song, J. (2020). North Pacific storm track response to the mesoscale SST in a global high-resolution atmospheric model. *Climate Dynamics*, *55*, 1597–1611. https://doi.org/10.1007/s00382-020-05343-x

Zuidema, P., Chang, P., Medeiros, B., Kirtman, B. P., Mechoso, R., Schneider, E. K., et al. (2016). Challenges and prospects for reducing coupled climate model SST biases in the eastern tropical Atlantic and Pacific Oceans: The U.S. CLIVAR Eastern tropical oceans synthesis working group. *Bulletin of the American Meteorological Society*, *97*, 2305–2328. https://doi.org/10.1175/bams-d-15-00274.1